Mutual Conservation of Redox Mediator and Singlet Oxygen Quencher in Lithium-Oxygen Batteries

Won-Jin Kwak,[1†] Stefan A. Freunberger,[2] Hun Kim,[1] Jiwon Park,[3] Trung Thien Nguyen,[1] Hun-Gi Jung,[4] Hye Ryung Byon,[3] Yang-Kook Sun[1,]*

1. Department of Energy Engineering, Hanyang University, Seoul 04763, Republic of Korea

2. Institute for Chemistry and Technology of Materials, Graz University of Technology, Graz 8010, Austria

3. Department of Chemistry, Korea Advanced Institute of Science and Technology (KAIST), and KAIST Institute for NanoCentury, Daejeon 34141, Republic of Korea

4. Center for Energy Convergence Research, Green City Technology Institute, Korea Institute of Science and Technology, Seoul 02792, Republic of Korea

[†]Present address: Energy & Environment Directorate, Pacific Northwest National Laboratory, Richland, Washington 99352, USA

KEYWORDS: Lithium oxygen batteries, Redox mediator, singlet oxygen, singlet oxygen quencher

ABSTARCT

Li-O_2 batteries are plagued by side reactions that cause poor rechargeability and efficiency. These reactions were recently revealed to be predominantly caused by singlet oxygen, which can be neutralized by chemical traps or physical quenchers. However, traps are irreversibly consumed and thus only active for limited time, and so far identified quenchers lack oxidative stability to be suitable for typically required recharge potentials. Thus, reducing the charge potential within the stability limit of the quencher and/or finding more stable quenchers is required. Here, we show that dimethylphenazine as a redox mediator decreases the charge potential well within the stability limit of the quencher 1,4-diazabicyclo[2.2.2]octane. The quencher can thus mitigate the parasitic reactions without being oxidatively decomposed. At the same time the quencher protects the redox mediator from singlet oxygen attack. The mutual conservation of the redox mediator and the quencher is rational for stable and effective Li-O_2 batteries.

1. INTRODUCTION

The high theoretical specific energy of non-aqueous lithium-oxygen (Li-O_2) batteries is based on the reversible formation and decomposition of lithium peroxide (Li_2O_2) upon discharge and charge.[1] However, practical realization requires overcoming many challenges. One of the most prominent challenges is the severe parasitic reactions that cause high charging potentials, poor rechargeability and cycle life.[2] For over a decade, electrolyte and electrode reactions with the reduced oxygen species, superoxide and peroxide, have been considered the primary source of the parasitic reactions.[3-5] However, reactions of reduced O_2 species with common electrolytes have been found to be thermodynamically unfavourable[6] and highly reversible cyclability of KO_2 in K-O_2 cells[7] demonstrates that other degradation pathways than superoxide attack must prevail. Only

recently has it been recognized that the highly reactive singlet oxygen ($^1O_2$), which has a quantum state in which all electrons are spin paired, predominantly causes the side reactions.[8-10] It was demonstrated that $^1O_2$ is produced during discharge and from the onset of charge, with the rate of $^1O_2$ increasing substantially with increasing charging potential or with trace H_2O to the electrolyte.[9] This pattern of $^1O_2$ abundance matches the degree of parasitic reactions in Li-O_2 cathodes. Furthermore, addition of $^1O_2$ traps or quenchers could substantially reduce side reactions[9]. This observation together with reversible K-O_2 cells [7] strongly suggests $^1O_2$ to be the dominant source of cathode deterioration.

To mitigate $^1O_2$ driven side reactions in Li-O_2 cells, 9,10-dimethylanthracene (DMA) and 1,4-diazabicyclo[2.2.2]octane (DABCO) have been shown to be effective chemical traps and physical quenchers, respectively. [9] At the level of $^1O_2$ abundance, however, DMA is consumed within a few cycles. DABCO has been proven to be highly capable of converting $^1O_2$ to $^3O_2$,[11] but is irreversibly oxidized above ~3.6 V, which is typically not sufficient to fully recharge the cell.[9]

To efficiently suppress the parasitic reaction caused by $^1O_2$, it is necessary to find more electrochemically stable quenchers and/or to lower the charge potential of Li-O_2 batteries within the stability window of quenchers. However, several representative quenchers known from biological systems[12-15] such as α-tocopherole and β-carotene are similarly to DABCO unstable in the required voltage range of Li-O_2 batteries (Figure. S1). Therefore, the charge potential has to be lowered, which may be achieved in two ways. One way is through solid catalysts, however, which also can enhance electrolyte decomposition and reduce the stability of DABCO.[16] The other way is using redox mediators that shuttle electron-holes between the porous electrode and the solid Li_2O_2. In this method, the mediator is oxidized at the electrode and then diffuses to the Li_2O_2, which is decomposed into O_2 and Li^+ by reforming the original reduced state of the mediator.[17-20]

This allows recharging the cell at rates and voltages that are by far impossible without the mediator. However, such mediators gradually degrade equally by attack of $^1O_2$ (Ref. 21). Furthermore, mediators may be unstable against lithium metal, which will require protection against direct contact.[22]

Here we show that quencher and mediator can work in synergy to neutralize $^1O_2$ and to lower the charge potential. We use the quencher DABCO to preserve the cell components including the mediator from $^1O_2$ attack in conjunction with the mediator 5,10-dihydro-5,10-dimethylphenazine (DMPZ) to reduce the charge potential well below the stability limit of DABCO. We verify also that the quencher protects the redox mediator from $^1O_2$ attack and allows thus for longer for efficient recharge. Thus, quencher and mediator gain their full potential only by mutually preserving each other as shown in **Scheme 1**.

2. EXPERIMENTAL METHODS

2.1. Materials

Diethylene glycol dimethyl ether (DEGDME, 99.5%), bis(trifluoromethane)sulfonimide lithium salt (LiTFSI, 99.95%), dimethylphenazine (DMPZ, ≥97%), 1,4-diazabicyclo[2.2.2]octane (DABCO, 99%), β-carotene (≥ 97%), α-tocopherol (≥ 96%), and acetonitrile (anhydrous, 99.8 %) were purchased from Sigma-Aldrich. Solvents were purified by distillation and further dried over activated molecular sieves until the final water content was < 10 ppm. DABCO and the mediators were recrystallized from absolute diethyl ether and ethanol, respectively, with molecular sieves present. The lithium salt was dried in a vacuum oven for 3 days at 140 °C. Moisture content of the solvents and electrolytes (without mediators or quencher present) was measured by Karl Fischer titration using a TitroLine KF trace (Schott). The sensitizer, palladium(II) meso-tetra(4-

fluorophenyl)tetrabenzoporphyrin (Pd4F), used for $^1O_2$ generation was synthesized in accordance with a previously reported procedure.[15] Glass fiber (GF/C, Whatman) was used as a separator after vacuum drying for 3 days at 180 °C. Using a filtration method, free standing multi-walled CNT (CM-150, Hanwha Chemical) electrode served as the working electrode (WE) without binder. Li metal foil (thickness: 200 μm) was purchased from Honjo Chemical and used as the counter and reference electrodes (CE and RE) which were protected by lithium-ion conductive glass-ceramics (LiCGC AG-01, Ohara).[22,23]

2.2. Cell assembly

Freestanding CNT was punched into circular pieces (1.2 cm in diameter) and dried at 80 °C under vacuum for 24 h. 1 M LiTFSI in DEGDME was prepared as the electrolyte, which was selectively mixed with the redox mediator (0.2 M, DMPZ) and singlet oxygen quencher (0.1 M, DABCO). To increase the possibility of quenching $^1O_2$ by DABCO and decomposing Li_2O_2 by DMPZ, suitable concentrations of redox mediator and singlet oxygen quencher had been considered and they were determined based on their solubility in DEGDME solvent. Cells were assembled using the dried CNT electrode (about 1.2 mg), glass fiber separator, Li metal, and the electrolyte in an Ar-filled glove box (water and oxygen content < 0.1 ppm). Closed coin type cells (CR2032, Welcos) were used for the CV test without O_2 gas, and homemade Li-O_2 cells[23] was used for the galvanostatic test under O_2. After cell assembly, Li-O_2 cells were stabilized under O_2 atmosphere (1.0 bar) for 1 h.

2.3. Electrochemical tests and analyses

The electrochemical tests were conducted using a VMP3 potentiostat (Biologic Instruments) for galvanostatic cycling with a current density of 0.12 mA (100 $mA \cdot g_C^{-1}$) and a time limit of 10 h in a voltage window of 2.0-4.8 V. For the rate capability test, the current density was changed, as noted in the chart, with the same total specific capacity.

UV-Vis absorption spectra were recorded on a Cary 50 UV-Vis spectrophotometer (Varian). $^1O_2$ was generated photochemically in O_2-saturated solution containing 1 μM of the photosensitizer palladium(II) *meso*-tetra(4-fluorophenyl)tetrabenzoporphyrin.[15] The process of photosensitization transfers photon energy via the sensitizer to $^3O_2$ and produces $^1O_2$. The sensitizer in the O_2-saturated solution with redox mediator or quencher was irradiated with a red light-emitting diode light source (643 nm, 7 W). During the measurement, electrolytes were stirred by a small magnetic bar in a cuvette to ensure uniform concentration of redox mediator, sensitizer, and oxygen species. The presence of Li_2O_2 was also confirmed by UV-Vis spectrometry via a titration method using titanium oxysulfate ($TiOSO_4$). The discharged and recharged working electrodes were added to the titration solution (2% $TiOSO_4$ in 0.1 M H_2SO_4) and shaken gently for 30 s. The concentration of the yellowish complex $[Ti(O_2)]^{2+}$, which is proportional to the Li_2O_2 concentration, was measured by analyzing the UV-Vis absorption spectra. ^{1}H-NMR was measured on a Varian VNMRS, 600 MHz spectrometer using DMSO-d_6. After the CV and galvanostatic tests, electrolytes were collected from the disassembled cell and diluted by DMSO-d_6 in Ar-filled glove box. The evolution of the discharge products on CNT electrodes were examined using field-emission scanning electron microscopy (FE-SEM, SUPRA 55VP, Carl Zeiss) and high-resolution X-ray diffraction (HR-XRD, 9 kW, SmartLab, Rigaku) with a Cu-Kα radiation source within a 2θ range of 30.0-60.0° at a scan rate of 1° min^{-1}. All the analyses for electrodes were performed after a careful washing procedure with the purified DEGDME solvent. Then, the sample was dried in

Ar-filled glove box and wrapped in vacuum-pack to prevent exposure in air during transfer to the analytical instrument for characterization.

To quantify the amount of carbonaceous by-products (Li_2CO_3 and Li carboxylates) formed at each stage of discharge and charge as shown in Figures 3d and e, the CNT electrodes were immersed in 1 M H_2SO_4 to decompose the present Li_2CO_3, followed by treatment with Fenton's reagent to oxidize the Li carboxylates, in accordance with established procedure in previous reports.[24,25] This procedure quantitatively separates Li_2CO_3 and Li carboxylates.

For the OEMS measurements, a custom-made OEMS cell was assembled with a Li metal film (Honjo) negative electrode, two pieces of separators (Celgard 2500 and GF/C glass fiber), and the freestanding CNT positive electrode in an Ar-filled glove box (MOTek, O_2 < 1 ppm, H_2O < 1 ppm). In this cell for OEMS analysis, the Li metal was protected by a non-reactive protective layer as reported in our previous report.[26] The setup reliably prevents contact of the electrolyte with the Li metal. A total 150 μL of electrolyte including 0.2 M DMPZ and 1 M LiTFSI in TEGDME, with or without 0.1 M DABCO was used. We employed TEGDME due to rapid evaporation of DEGDME in an OEMS cell. The OEMS consisting of a 6-way and 2-position valve has periodically switched the valve to inject the gas, which was integrated in an OEMS cell for ~30 min, to a residual gas analyzer (RGA 200, Stanford Research Systems). The pressure change in an OEMS cell was also concurrently recorded during discharge and recharge using a high precision pressure transducer (Omega Engineering) to quantitatively analyze gas species. The electrochemical examinations for OEMS analysis were carried out using a potentiostat (VERSASTAT3, Princeton applied research).

3. RESULTS AND DISCUSSION

3.1. Prevention of quencher oxidation by redox mediator

Oxidation of DABCO shows an onset potential of ~3.5 V in our experiment which is much lower than typical charge potential of Li-O_2 batteries (> 4 V) comprising carbon electrodes and an organic electrolyte as shown in Figure 1a. This value is similar to the previously reported one in tetraethyleneglycol dimethyl ether,[9] the slight difference could be because of the different electrolyte. To avoid reactions of mediators with Li metal, their contact was prevented by a lithium-ion conductive glass-ceramic as a separator (LiCGC, Ohara) for all the cells in our study. The detailed setup was reported previously.[22,23]

DABCO oxidation is irreversible, as indicated by the missing reduction peaks. To effectively use DABCO, the recharge potential needs be maintained below 3.4 V. To meet this requirement, we used DMPZ as a redox mediator because of its redox potential being below the irreversible oxidation potential of DABCO. LiI could be another frequently used candidate with similarly low oxidation potential but we dismissed it due to complex side reactions and various discharge products.[27,28] Moreover, compared to other redox mediators, DMPZ was considered based on its low potential in combination with high stability against superoxide as shown previously.[20] Figure 1a shows the reversible redox behavior of DMPZ/$DMPZ^+$ in comparison with DABCO oxidation, suggesting that DMPZ/$DMPZ^+$ mediated Li_2O_2 oxidation is well within the stability window of DABCO. To check the decomposition of DABCO at the high charge potential, we analyzed the electrolytes after the CV tests by ^{1}H-NMR (Figure 1b). DABCO remained unaffected up to 3.4 V, which is sufficient to oxidize DMPZ. Hence, NMR data of the electrolyte containing both DMPZ and DABCO, after a CV test up to 3.4 V, confirmed that DMPZ/$DMPZ^+$ does not equally decompose DABCO (blue line in Figure 1b). However, at an oxidation potential of 4.3 V, which is typically required to charge a cell without a mediator, the decreasing peak for DABCO and new

peak for byproducts due to irreversible decomposition could be seen in the NMR (red line in Figure 1b). NMR spectra before CV tests for electrolytes with or without additives are supplied in Figure S2.

3.2. Li-O_2 cell cycling

Figure 2a compares the galvanostatic discharge/charge curves of Li-O_2 cells with and without additives. Based on the electrochemical stability of DABCO, unstable (red) and stable (blue) regions are separated. A recharge plateau of ~3.2 V with DMPZ as a mediator in accord with previous studies[20,22] is well within the safe region of DABCO. In other words, DMPZ reduces the charge potential into a range where DABCO can protect the cell against $^1O_2$. Voltage profiles of Li-O_2 batteries with an electrolyte that contains both DMPZ and DABCO demonstrate the synergy of the additives for 50 cycles whereas a cell with DABCO alone as additive exhibits continuous and irreversible quencher oxidation as indicated by the diminishing plateau at ~3.4 V (Figure 2b). In addition, DMPZ alone is ineffective for extended cycling as shown in Figure S3. The low charge potential plateau found in early cycles gives way to a recharge voltage above 4 V within only 10 cycles as a result of DMPZ decomposition and resembles a cell without a mediator (Figure S3). Such a gradual deactivation of redox mediators has been noticed before[22,23,29,30] and has been recently shown to be caused by $^1O_2$,[21] which produces parasitic gases like H_2 and CO. As another evidence for synergy effect of DMPZ and DABCO, we found that voltage profiles of Li-O_2 cell using only DMPZ exhibit two voltage plateaus during discharge from the second cycle onwards. This indicates that the electrochemically oxidized DMPZ did not fully react with Li_2O_2 on charge in the previous cycle. Therefore, the absence of the higher plateau in Li-O_2 cell with DMPZ and

DABCO means that DABCO suppresses side reaction from $^1O_2$ and makes Li_2O_2 oxidation by DMPZ more efficient.

Figure 2c shows the round trip efficiency which means the ratio of energy density during discharge to energy density during charge of the Li-O_2 cells. Although the efficiency of all cells decreases during the cycling test, the cell with DMPZ + DABCO electrolyte cycled by far for the most cycles.

Remaining efficiency decrease may be ascribed to electrode surface passivation and pores clogging at the cathode, caused by side reactions between Li_2O_2 or superoxide and electrolyte or minor unquenched $^1O_2$.[16] Thereby, the slight reduction in the efficiency during 50 cycles observed in Figure 2c indicates the need for the development of more stable electrolyte solvents at the cathode side, which requires further study. Taken together, the redox mediator DMPZ and the quencher DABCO act in combination to reduce the charge potential and protect the mediator against $^1O_2$ for either additive to preserve its effect over extended cycling as suggested by the voltage profiles. These effects are corroborated below by spectroscopic means.

We investigated the discharge and charge with quencher and mediator by UV-Vis, SEM, and XRD (Figure S4). UV-Vis data of discharged and recharged electrodes immersed in Ti^{4+} solution reveal the formation and decomposition of the peroxide product.[31] This is in accord with XRD data that show Li_2O_2 as the only crystalline product, as well as with visual inspection by SEM that shows the reconstitution of a clean electrode after recharge. These data demonstrate that Li-O_2 batteries with redox mediator and quencher cycle predominantly by the formation/decomposition of Li_2O_2.

High rates raise charge potentials even when a mediator is employed. To test this, we cycled the cell with mediator and quencher at various rates up to 500 $mA \cdot g_C^{-1}$ which shows that even at this high rate the charge potential stays well below the oxidation potential of DABCO (Figure 2d). The results above suggest that mediator and quencher in Li-O_2 cells preserve each other mutually.

An important goal with Li-O2 cells is to achieve extended cyclability with deep discharge. While data for deep discharge without and with quencher (Fig. SX) indicate improvement in recharge efficiency with quencher, cyclability is only marginally increased, which deserves deeper discussion. What a quencher can do is to mitigate 1O2 related chemical decomposition of cell components. To the best of our knowledge there is no reason to assume that the extent of side reactions changes over the depth of discharge. Therefore, the amount of side products scales with the charge passed. That this is true is reported in a number of independent studies as, for example, by McCloskey et al. [Ref J. Phys. Chem. Lett. 2013, 4, 2989] in Fig. R1.1. Furthermore, our own data in Fig. 3e show the amount of side products versus depth of discharge and confirms linear increase. Turning to charge, it is now well recognized that side products are also produced on charge with the rate growing as voltage increases and some of the solid products being oxidized towards the end of charge.[, *J. Phys. Chem. Lett.*, 2012, **3**, 3043-3047. , *J. Am. Chem. Soc.*, 2013, **135**, 494-500.] If anything, successive recharge after shallow cycling will rather increase the cumulative side products formed on charge in comparison to a full discharge/charge cycles with the same total discharge and charge capacity of multiple shallow cycles.

A prominent reason why shallow cycling is often pursued is to avoid limitations of rechargeability because of possible mechanical degradation of the porous electrode by the large amounts of Li_2O_2 formed upon deep discharge. This reason of degradation can certainly not be

mitigated by a quencher. The important metric showing the benefit of the cell with quencher in comparison to the cell with mediator alone is the degradation over cumulative discharge/charge capacity. Since we cycle all cell configurations in Fig. 2 with the same constant capacity, cumulative capacity simply scales with cycle number. Fig. 2c shows the major improvement with DABCO in comparison to the other configurations. Clearly, there is still degradation, but it is clear that $^1O_2$ is not the only source of degradation and therefore the quencher cannot completely mitigate degradation. Complete abolishment of degradation cannot be expected since there are other reasons for fading than side products caused by $^1O_2$. These degradation mechanisms appear to particularly strongly kick in with deeper discharge. Shallow cycling is hence a viable way to achieve larger cumulative capacity to study the impact of mediator and quencher on chemical degradation by $^1O_2$. Overall, the comparison of quencher/mediator combinations with other configurations demonstrate the major benefit of this combination.

3.3. Protection of redox mediator by quencher from $^1O_2$ attack

While it is clear that the lower charge potential with a mediator inhibits the electrochemical oxidation of DABCO, the effect of the quencher on DMPZ requires additional proof. To do this, we exposed the DMPZ to $^1O_2$ in the absence or presence or DABCO, and recorded the DMPZ concentration over time by UV-Vis, as shown in Figures 3a and b. $^1O_2$ was generated in-situ by photosensitation reaction as described in experimental section.

In the absence of quencher, the DMPZ concentration continuously decreased when $^1O_2$ was generated, which means that $^1O_2$ deactivates DMPZ and thus, degrades the efficacy of the DMPZ/DMPZ$^+$ couple (Figure 3a). However, with quencher in the electrolyte, the DMPZ

concentration remained unchanged (Figure 3b). Therefore, the quencher preserves the RM from $^1O_2$ attack. To prove this shielding effect of DABCO for DMPZ from the $^1O_2$ attack in Li-O_2 batteries, we recorded ^{1}H-NMR spectra of electrolytes containing either DMPZ only or DMPZ and DABCO after Li-O_2 cell cycling (Figure 3c). The peaks for DMPZ disappeared (methyl at 2.97 ppm, aromatic Hs at ~6.7 ppm) after 50 cycles without DABCO. However, with DABCO, peaks from DABCO and DMPZ were largely preserved. DMPZ is nevertheless decomposed due to inherent instability as seen by the H_2 evolution. Whilst not clarified in detail, this decomposition appears not to produce new by-products that are visible in the NMR.

Given that $^1O_2$ formation has been shown before to occur during both discharge and charge, DABCO and DMPZ may be expected to improve recharge as well as discharge. To prove this, we quantified the amount of carbonaceous side products (lithium carbonate and carboxylates) formed at various states of discharge and charge. The electrodes were analyzed with a previously reported procedure,[24,25] involving the treatment of washed electrodes with acid to decompose the present Li_2CO_3, followed by treatment with Fenton's reagent to oxidize the Li carboxylates. The evolved CO_2 was quantified by mass spectrometry, and the results are presented in Figure 3e together with the sample points along the cycling curve indicated in Figure 3d. Considering first the cell with DMPZ alone (red curve), the amount of side products roughly scales with the depth of discharge. As the cell is charged, the amount further increases up to half recharge and then decreases as the cell reaches full recharge. This behavior can be explained by the fact that charging, Li-O_2 cells produce significantly more $^1O_2$ from the onset of charge than on discharge.[9] As charging progresses towards full recharge, the side products appear to be also partly oxidized. The addition of DABCO significantly reduces the amount of side products throughout the entire cycle, compared with the cell without DABCO. These results mean that $^1O_2$ provokes parasitic reactions

to form by-products regardless of redox mediator, but the quenching effect of DABCO can partly mitigate these parasitic reactions (decomposition of redox mediator and electrolyte solvent),[8,9] which is in good agreement with UV-Vis, GC-MS and H-NMR data with or without DABCO (Figure 3).

We could also confirm the formation of a certain amount of by-products despite the simultaneous use of DABCO and DMPZ in the Li-O_2 cell. The byproducts are carbonaceous side reaction products (lithium acetate, formate and carbonate) as previously reported.[16,24,25] Reasons include both incomplete quenching of $^1O_2$ by DABCO and the side reaction triggered by the reduced oxygen species LiO_2 and Li_2O_2 with the electrolyte (solvent, salt, and additives) as confirmed in previous reports.[16,32]

Finally, we used on-line electrochemical mass spectrometry (OEMS) to investigate the effect of combined RM and quencher on the O2 evolution efficiency, Figure 4. During discharge the e^-/O_2 ratios were 2.02 e^-/O_2 for the combination of DABCO and DMPZ, and 2.10 e^-/O_2 for DMPZ only. The e^-/O_2 ratio with DABCO being closer to the ideal value of 2 indicates less side reaction in the presence of $^1O_2$ quencher. During recharge, the quantity of O_2 evolving is higher with DABCO and DMPZ (blue, 7.45 μmol, 6.03 e^-/O_2) than that with DMPZ alone (red, 5.26 μmol, 8.52 e^-/O_2), which also goes along with lower recharge voltage with DABCO. In addition, the relative amount of H_2 evolving is smaller for the cell containing DMPZ and DABCO (Figure S5). It is worth noting that the H_2 gas evolves for both cells presumably due to decomposition of DMPZ at the positive electrode as reported previously.[33] However, DMPZ is stabilized in the presence of DABCO, which causes better O_2 evolution efficiency. CO_2 evolution was observed for neither cell (Figure S5), likely because DMPZ keeps the charge potential below 3.5 V, which is below the onset of side product decomposition at ~3.8 V. [10, insert also *J. Am. Chem. Soc.*, 2011, **133**, 8040] Taken all together, the

OEMS results highlight the important role of the $^1O_2$ quencher to retain the efficiency of the redox mediator for longer than is the case without quencher. Our results also motivate further studies with DMPZ as it may possibly lead to more general insights into how RMs should be designed with consideration of stability. In addition, the stability of O_2 reduction mediators and any other possibly attacked component against $^1O_2$ should be considered as well.[34,35]

4. CONCLUSION

In summary, $^1O_2$ quenchers suitable for Li-O_2 cells show an oxidation stability that is below the typically required recharge potential beyond 4 V vs. Li/Li^+. Thus, using them during cycling requires redox mediators to reduce the charge potential. In turn, the quencher can mitigate the frequently observed degradation of the redox mediator and of other cell components by $^1O_2$. The chosen pairing of quencher and mediator serves well to demonstrate the principle, and the mutual cooperation of key components provides an overall rational strategy toward more stable and efficient Li-O_2 batteries. This study points out more generally that components can alleviate each other's deficiencies, to create optimal effects for redox mediator and singlet oxygen quencher, rather than just a combination.

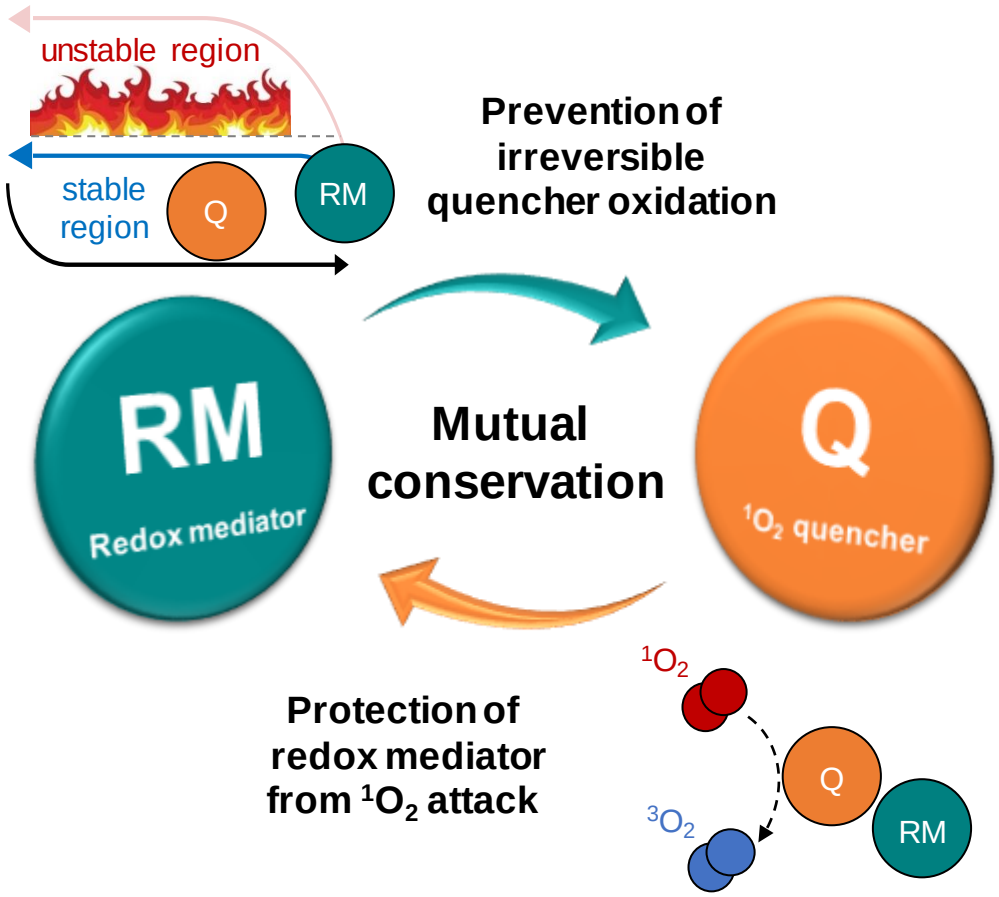

Scheme 1. Schematic illustration of the mutual conservation of redox mediator (RM) and singlet oxygen quencher (Q) in a Li-O_2 battery system.

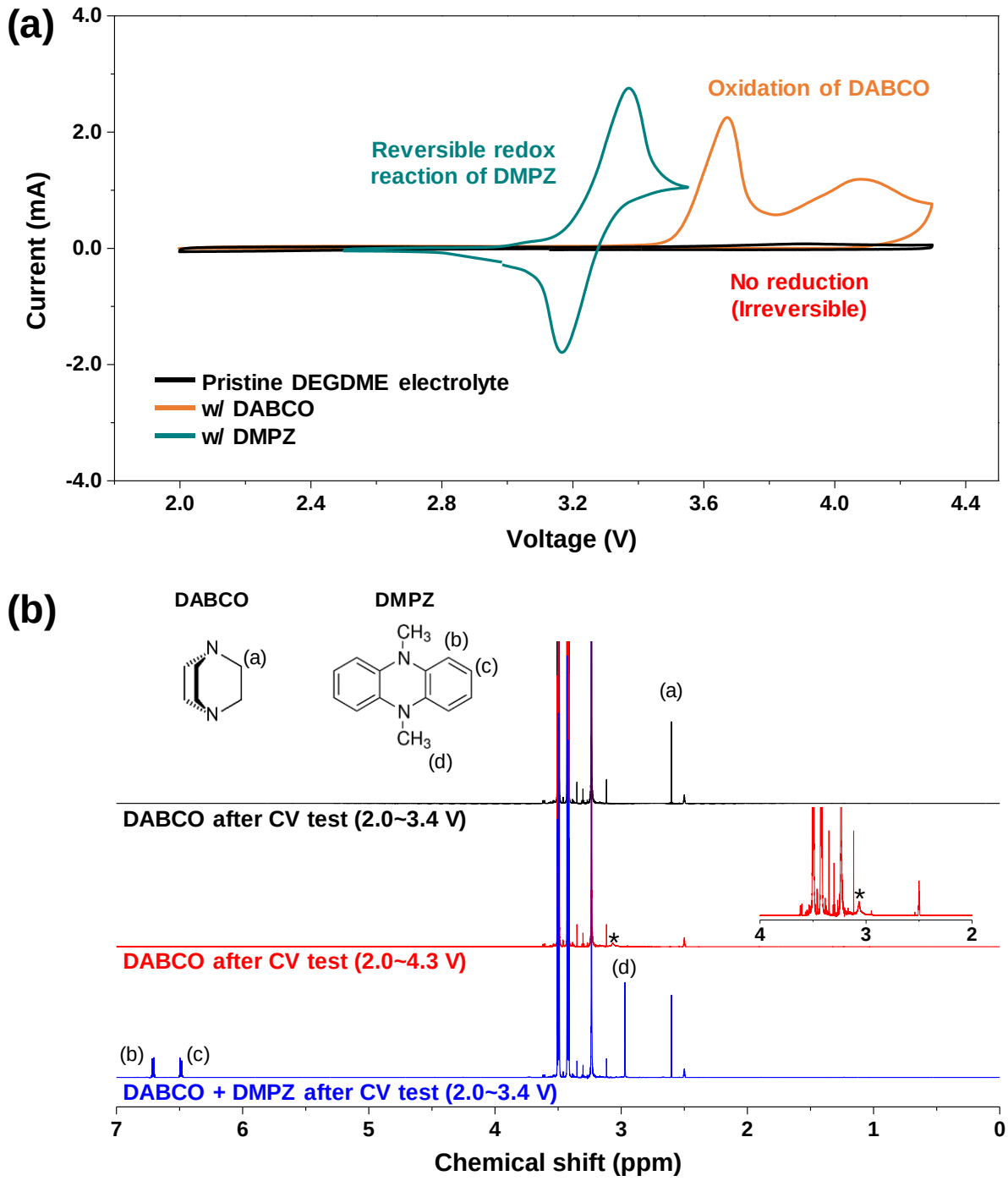

Figure 1. Oxidation instability of DABCO as $^1O_2$ quencher and reversible redox reaction of DMPZ as redox mediator. (a) Voltammograms (1.0 mV s^{-1}) using 1 M LiTFSI in diethylene glycol dimethyl ether (DEGDME) solutions without and with DABCO or DMPZ, respectively, under Ar

atmosphere. (b) ^{1}H-NMR spectra (in DMSO-d_6) for electrolytes after 1st cycle CV tests over different voltage ranges (2.0-3.4 V and 2.0-4.3 V) for checking the decomposition of DABCO by irreversible oxidation. Insets for each spectrum are the same data to avoid overlays of data. The * denotes a decomposed DABCO after irreversible oxidation.

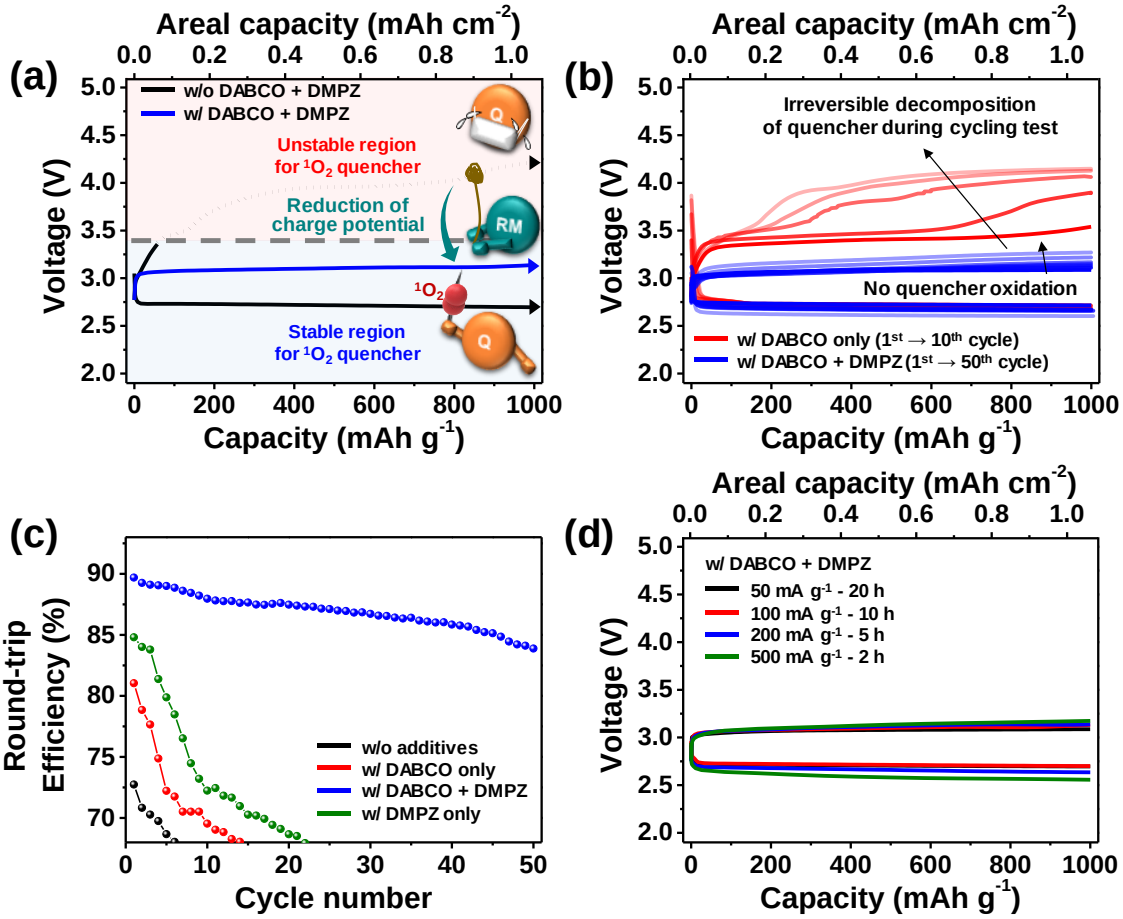

Figure 2. Cycling behavior of Li-O_2 batteries with different electrolytes. (a) Voltage profile of Li-O_2 batteries with and without additives (DABCO + DMPZ) at 100 mA·g_C^{-1}. (b) Galvanostatic cycling of Li-O_2 batteries with a DEGDME/1 M LiTFSI electrolyte containing only DABCO or DABCO + DMPZ at 100 mA·g_C^{-1}. (c) Round-trip efficiencies versus cycle number. The efficiency is the ratio between the discharge and charge energy as obtained by integrating the voltage over the capacity. Cells were cycled at a fixed capacity of 1000 mAh·g_C^{-1} (1.061 mAh cm^{-2}) and a constant current of 100 mA·g_C^{-1}. The voltage limits were 2.0 and 4.8 V, but none of the cells reached these limits during these experiments. (d) Rate capability with an electrolyte containing DABCO and DMPZ. The times given in the label denote the time per half cycle.

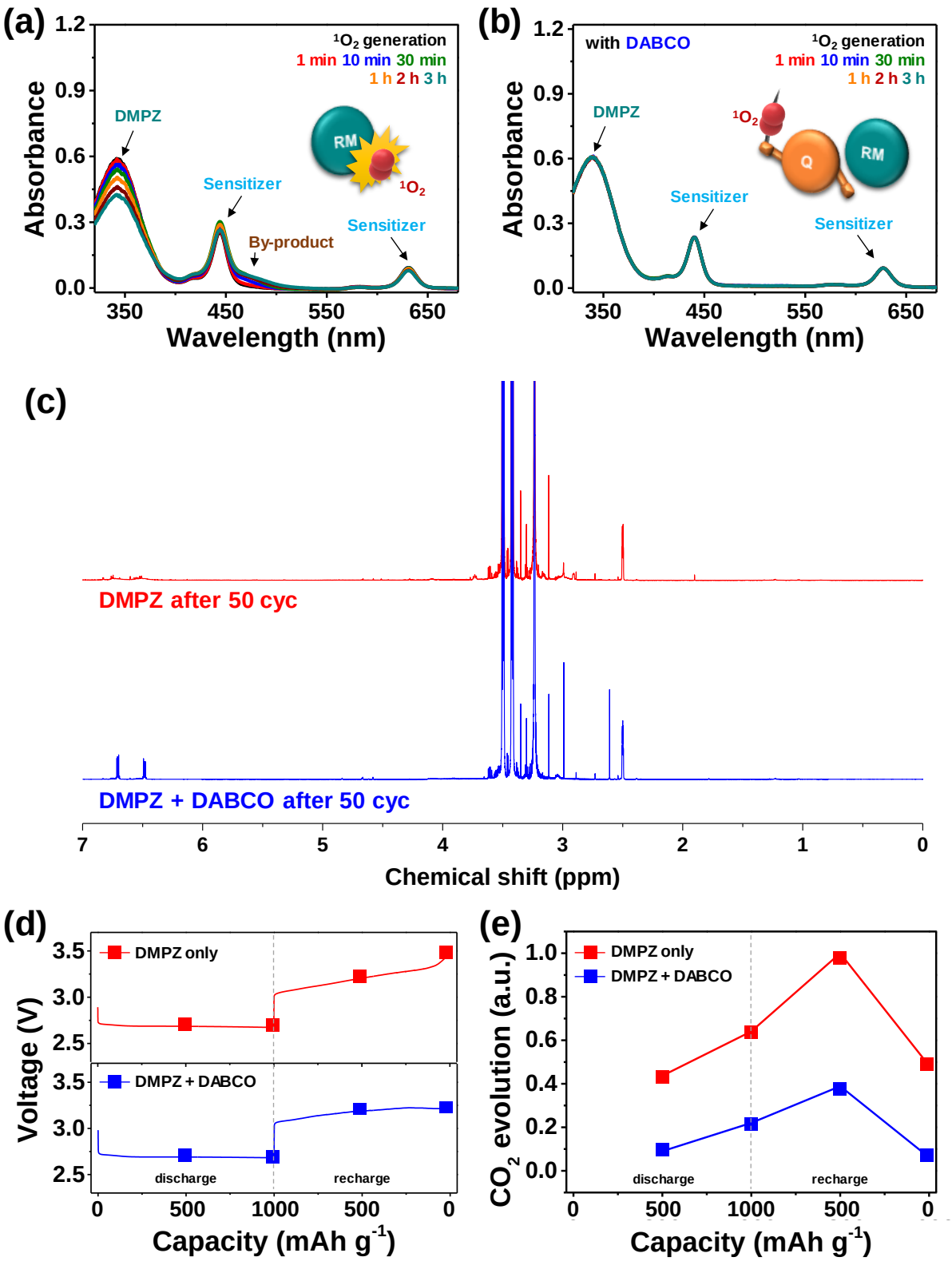
(a)
Absorbance
Wavelength (nm)
$^1O_2$ generation
1 min 10 min 30 min
1 h 2 h 3 h
DMPZ
Sensitizer
By-product
Sensitizer
RM
$^1O_2$
(b)
with DABCO
$^1O_2$ generation
1 min 10 min 30 min
1 h 2 h 3 h
DMPZ
Sensitizer
Sensitizer
$^1O_2$
Q
RM
(c)
DMPZ after 50 cyc
DMPZ + DABCO after 50 cyc
Chemical shift (ppm)
(d)
DMPZ only
DMPZ + DABCO
Voltage (V)
discharge
recharge
Capacity (mAh g^{-1})
(e)
DMPZ only
DMPZ + DABCO
CO_2 evolution (a.u.)
discharge
recharge
Capacity (mAh g^{-1})

Figure 3. Analysis for checking the effect of DABCO to protect DMPZ and Li-O_2 cells from $^1O_2$. UV-Vis data of DMPZ electrolyte after $^1O_2$ generation (a) without and (b) with DABCO. Peaks at 444 and 630 nm stem from the sensitizer to generate $^1O_2$. (c) ^{1}H-NMR spectra (in DMSO-d_6) for checking stability of DMPZ in electrolytes containing either no additive, or DABCO after Li-O_2 cell tests (50th cycle). (d,e) Ex-situ analysis of by-products in Li-O_2 batteries using DMPZ or DMPZ + DABCO. (d) Representative voltage profile during galvanostatic discharge and charge of Li-O_2 cells. Cells were stopped at the points indicated, the electrodes washed and carbonaceous side reaction products analyzed. (e) Relative amount of carbonaceous side reaction products analyzed by GC-MS at the indicated states of charge.

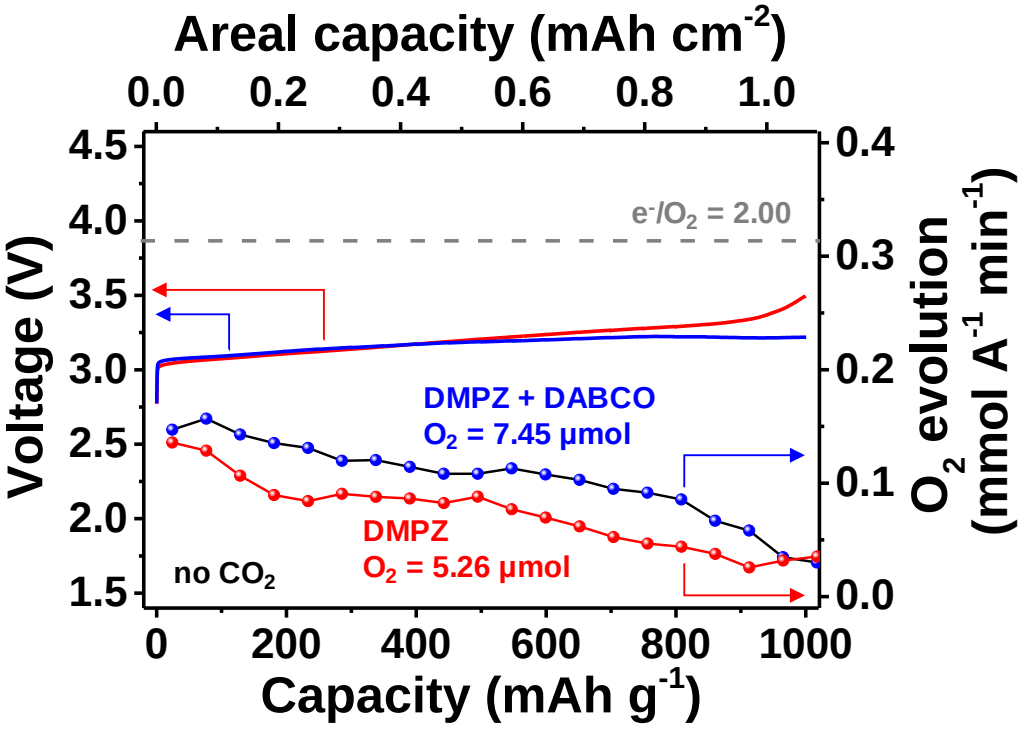

Figure 4. On-line electrochemical mass spectrometry (OEMS). OEMS analysis of Li-O_2 cells with electrolytes (1 M LiTFSI in TEGDME) containing 0.2 M DMPZ only (red) or 0.1 M DABCO with DMPZ (blue). Voltage profiles and O_2 evolution rates were concurrently measured after the cells were discharged to 1000mAh g^{-1} at 100 mA g^{-1}.

■ ASSOCIATED CONTENT

Corresponding Author

*E-mail: yksun@hanyang.ac.kr

Author Contributions

Won-Jin Kwak,[1†] Stefan A. Freunberger,[2] Hun Kim,1 Jiwon Park,[3] Trung Thien Nguyen,[1] Hun-Gi Jung,[4] Hye Ryung Byon,[3] Yang-Kook Sun[1,*]

Present Addresses

1. Department of Energy Engineering, Hanyang University, Seoul 04763, Republic of Korea

2. Institute for Chemistry and Technology of Materials, Graz University of Technology, Graz 8010, Austria

3. Department of Chemistry, Korea Advanced Institute of Science and Technology (KAIST), and KAIST Institute for NanoCentury, Daejeon 34141, Republic of Korea

4. Center for Energy Convergence Research, Green City Technology Institute, Korea Institute of Science and Technology, Seoul 02792, Republic of Korea

[†]Present address: Energy & Environment Directorate, Pacific Northwest National Laboratory, Richland, Washington 99352, USA

Notes

The authors declare no competing financial interest.

Supporting Information

^{1}H-NMR for electrolyte. Electrochemical test result. Analysis of discharge product; UV-Vis titration, XRD patterns and SEM image for cathode. The Supporting Information is available free of charge on the ACS Publications website at DOI:

■ ACKNOWLEDGMENT

This work was supported by a Human Resources Development program (No. 20184010201720) of a Korea Institute of Energy Technology Evaluation and Planning (KETEP) grant, funded by the Ministry of Trade, Industry and Energy of the Korean government, and supported by National Research Foundation of Korea (NRF) grant funded by the Korea government Ministry of Education and Science Technology (MEST) (NRF-2016R1C1B2008690). S.A.F. is indebted to the European Research Council (ERC) under the European Union's Horizon 2020 research and innovation programme (grant agreement No 636069).

■ REFERENCES

(1) Jung, H.-G.; Hassoun, J.; Park, J.-B.; Sun, Y.-K.; Scrosati, B. An improved high-performance lithium–air battery. *Nat. Chem.* **2012**, *4*, 579-585.

(2) Aurbach, D.; McCloskey, B. D.; Nazar, L. F.; Bruce, P. G. Advances in understanding mechanisms underpinning lithium–air batteries. *Nat. Energy* **2016**, *1*, 16128.

(3) McCloskey, B. D.; Speidel, A.; Scheffler, R.; Miller, D. C.; Viswanathan, V.; Hummelshøj, J. S.; Nørskov, J. K.; Luntz, A. C. Twin Problems of Interfacial Carbonate Formation in Nonaqueous Li–O_2 Batteries. *J. Phys. Chem. Lett.* **2012**, *3*, 997-1001.

(4) Black, R.; Oh, S. H.; Lee, J.-H.; Yim, T.; Adams, B.; Nazar, L. F. Screening for Superoxide Reactivity in Li-O_2 Batteries: Effect on Li_2O_2/LiOH Crystallization. *J. Am. Chem. Soc.* **2012**, *134*, 2902-2905.

(5) Bryantsev, V. S.; Giordani, V.; Walker, W.; Blanco, M.; Zecevic, S.; Sasaki, K.; Uddin, J.; Addison, D.; Chase, G. V. Predicting Solvent Stability in Aprotic Electrolyte Li–Air Batteries: Nucleophilic Substitution by the Superoxide Anion Radical ($O_2^{\bullet-}$). *J. Phys. Chem. A* **2011**, *115*, 12399-12409.

(6) Mahne, N.; Fontaine, O.; Thotiyl, M. O.; Wilkening, M.; Freunberger S. A. Mechanism and performance of lithium–oxygen batteries – a perspective. *Chem. Sci.* **2017**, *8*, 6716-6729.

(7) Cong, G.; Wang, W.; Lai, N.-C.; Liang, Z.; Lu, Y.-C. A high-rate and long-life organic–oxygen battery. *Nat. Mater.* **2019**, *18*, 390-396.

(8) Wandt, J.; Jakes, P.; Granwehr, J.; Gasteiger, H. A.; Eichel, R.-A. Singlet oxygen formation during the charging process of an aprotic lithium–oxygen battery. *Angew. Chem. Int. Ed.* **2016**, *55*, 6892-6895.

(9) Mahne, N.; Schafzahl, B.; Leypold, C.; Leypold, M.; Grumm, S.; Leitgeb, A.; Strohmeier, G. A.; Wilkening, M.; Fontaine, O.; Kramer, D.; Slugovc, C.; Borisov, S. M.; Freunberger, S. A. Singlet oxygen generation as a major cause for parasitic reactions during cycling of aprotic lithium–oxygen batteries. *Nat. Energy* **2017**, *2*, 17036.

(10) Mahne, N.; Renfrew Sara, E.; McCloskey Bryan, D.; Freunberger Stefan, A. Electrochemical oxidation of lithium carbonate generates singlet oxygen. *Angew. Chem. Int. Ed.* **2018**, *57*, 5529-5533.

(11) Khan, A. U. Theory of Electron Transfer Generation and Quenching of Singlet Oxygen [$^1\sum_g^+$ and $^1\Delta_g$] by Superoxide Anion. The Role of Water in the Dismutation of O_2^-. *J. Am. Chem. Soc.* **1977**, *99*, 370-371.

(12) Krieger-Liszkay, A.; Trebst, Achim. Tocopherol is the scavenger of singlet oxygen produced by the triplet states of chlorophyll in the PSII reaction centre. *J. Exp. Bot.* **2006**, *57*, 1677-1684.

(13) Baltschun, D.; Beutner, S.; Briviba, K.; Martin, H.-D.; Paust, J.; Peters, M.; Röver, S.; Sies, H.; Stahl, W.; Steigel, A.; Stenhorst, F. Singlet oxygen quenching abilities of carotenoids. *Liebigs Annalen* **1997**, *1997*, 1887-1893.

(14) Corey, E. J.; Mehrotra, M. M.; Khan, A. U. Water induced dismutation of superoxide anion generates singlet molecular oxygen. *Biochem. Biophys. Res. Commun.* **1987**, *145*, 842-846.

(15) Borisov, S. M.; Nuss, G.; Haas, W.; Saf, R.; Schmuck, M.; Klimant, I. New NIR-emitting complexes of platinum (II) and palladium (II) with fluorinated benzoporphyrins. *J. Photochem. Photobiol. A* **2009**, *201*, 128-135.

(16) Wong, R. A.; Yang, C.; Dutta, A.; O, M.; Hong, M.; Thomas, M. L.; Yamanaka, K.; Ohta, T.; Waki, K.; Byon, H. R. Critically Examining the Role of Nanocatalysts in Li–O_2 Batteries: Viability toward Suppression of Recharge Overpotential, Rechargeability, and Cyclability. *ACS Energy Lett.* **2018**, *3*, 592-597.

(17) Bergner, B. J.; Schürmann, A.; Peppler, K.; Garsuch, A.; Janek, J. TEMPO: A Mobile Catalyst for Rechargeable Li-O_2 Batteries. *J. Am. Chem. Soc.* **2014**, *136*, 15054-15064.

(18) Chen, Y.; Freunberger, S. A.; Peng, Z.; Fontaine, O.; Bruce, P. G. Charging a Li–O_2 battery using a redox mediator. *Nat. Chem.* **2013**, *5*, 489-494.

(19) Kwak, W.-J.; Hirshberg, D.; Sharon, D.; Afri, M.; Frimer, A. A.; Jung, H.-G.; Aurbach, D.; Sun, Y.-K. Li–O_2 cells with LiBr as an electrolyte and a redox mediator. *Energy Environ. Sci.* **2016**, *9*, 2334-2345.

(20) Lim, H.-D.; Lee, B.; Zheng, Y.; Hong, J.; Kim, J.; Gwon, H.; Ko, Y.; Lee, M.; Cho, K.; Kang, K. Rational design of redox mediators for advanced Li–O_2 batteries. *Nat. Energy* **2016**, *1*, 16066.

(21) Kwak, W.-J.; Kim, H.; Nguyen1, T. T.; Petit, Y. K.; Mahne, N.; Leypold, C; Redfern, p.; Curtiss, L. A.; Jung, H.-G.; Borisov, S. M.; Freunberger, S. A.; Sun, Y.-K. Deactivation of redox mediators in lithium-oxygen batteries by singlet oxygen. *Nat. Commun.* **2019,** *10*, 1380.

(22) Kwak, W.-J.; Jung, H.-G.; Aurbach, D.; Sun, Y.-K. Optimized Bicompartment Two Solution Cells for Effective and Stable Operation of Li–O_2 Batteries. *Adv. Energy Mater.* **2017**, *7*, 1701232.

(23) Kwak, W.-J.; Kim, H.; Jung, H.-G.; Aurbach, D.; Sun, Y.-K. A Comparative Evaluation of Redox Mediators for Li-O_2 Batteries: A Critical Review. *J. Electrochem. Soc.* **2018**, *165*, A2274-A2293.

(24) Ottakam Thotiyl, M. M.; Freunberger, S. A.; Peng, Z.; Bruce, P. G. The Carbon Electrode in Nonaqueous Li–O_2 Cells. *J. Am. Chem. Soc.* **2013**, *135*, 494-500.

(25) Schafzahl, B.; Mourad, E.; Schafzahl, L.; Petit, Y. K.; Raju, A. R.; Thotiyl, M. O.; Wilkening, M.; Slugovc, C.; Freunberger, S. A. Quantifying Total Superoxide, Peroxide, and

Carbonaceous Compounds in Metal–O_2 Batteries and the Solid Electrolyte Interphase. *ACS Energy Letters* **2018**, *3*, 170-176.

(26) Kwak, W.-J.; Park, J.; Nguyen, T. T.; Kim, H.; Byon, H. R.; Jang, M.; Sun, Y.-K. Dendrite- and Oxygen-Proof Protective Layer for Lithium Metal in Lithium-Oxygen Batteries. *J. Mater. Chem. A* **2019**, *7*, 3857-3862.

(27) Kwak, W.-J.; Hirshberg, D.; Sharon, D.; Shin, H.-J.; Arfi, M.; Park, J.-B.; Garsuch, A.; Chesneau, F. F.; Frimer, A. A.; Aurbach, D.; Sun, Y.-K. Understanding the behavior of Li–oxygen cells containing LiI. *J. Mater. Chem. A* **2015**, *3*, 8855-8864.

(28) Tułodziecki, M.; Leverick, G. M.; Amanchukwu, C. V.; Katayama, Y.; Kwabi, D. G.; Barde, F.; Hammond, P. T.; Shao-Horn, Y. The role of iodide in the formation of lithium hydroxide in lithium–oxygen batteries. *Energy Environ. Sci.* **2017**, *10*, 1828-1842.

(29) Bergner, B. J.; Busche, M. R.; Pinedo, R.; Berkes, B. B.; Schröder, D.; Janek, J. How To Improve Capacity and Cycling Stability for Next Generation Li–O_2 Batteries: Approach with a Solid Electrolyte and Elevated Redox Mediator Concentrations. *ACS Appl. Mater. Interf.* **2016**, *8*, 7756-7765.

(30) Kwak, W.-J.; Park, S.-J.; Jung, H.-G.; Sun, Y.-K. Optimized Concentration of Redox Mediator and Surface Protection of Li Metal for Maintenance of High Energy Efficiency in Li–O_2 Batteries. *Adv. Energy Mater.* **2018**, *8*, 1702258.

(31) Hartmann, P.; Bender, C. L.; Sann, J.; Durr, A. K.; Jansen, M.; Janek, J.; Adelhelm, P. A comprehensive study on the cell chemistry of the sodium superoxide (NaO_2) battery. P. *Phys. Chem. Chem. Phys.* **2013**, *15*, 11661-11672.

(32) Wang, Y.; Lai, N.-C.; Lu, Y.-R.; Zhou, Y.; Dong, C.-L.; Lu, Y.-C. A Solvent-Controlled Oxidation Mechanism of Li_2O_2 in Lithium-Oxygen Batteries. *Joule* **2018**, *2*, 2364-2380.

(33) Liang, Z.; Lu, Y.-C.; Critical role of redox mediator in suppressing charging instabilities of lithium–oxygen batteries. *J. Am. Chem. Soc.* **2016**, *138*, 7574-7583.

(34) Gao, X.; Chen, Y.; Johnson, L.; Bruce, P. G. Promoting solution phase discharge in Li–O_2 batteries containing weakly solvating electrolyte solutions. *Nat. Mater.* **2016**, *15*, 882-886.

(35) Qiao, Y.; He, Y.; Wu, S.; Jiang, K.; Li, X.; Guo, S.; He, P.; Zhou, H. MOF-Based Separator in an Li–O_2 Battery: An Effective Strategy to Restrain the Shuttling of Dual Redox Mediators. *ACS Energy Lett.* **2018**, *32*, 463-468.

BRIEF: In this study, the chosen pairing of quencher and mediator serves well to demonstrate the principle and mutual cooperation of key components gives overall a rational strategy towards stable and efficient Li-O_2 batteries.

Table of Contents (TOC) abstract graphic: